Planetary Nebulae: A Universal Toolbox in the Era of Precision Astrophysics
Proceedings IAU Symposium No. 384, 2025
O. De Marco, A. Zijlstra & R. Szczerba, eds.
doi:10.1017/S1743921324000954

Nova remnants ... the fast siblings of planetary nebulae

Martín A. Guerrero[1] **and Edgar I. Santamaría**[2]

[1]Instituto de Astrofísica de Andalucía, IAA-CSIC, Glorieta de la Astronomía s/n, E-18008 Granada, Spain

[2]Instituto de Radioastronomía y Astrofísica (IRyA), UNAM Campus Morelia, Apartado postal 3-72, 58090 Morelia, Michoacán, Mexico

Abstract. Classical and recurrent novae are luminous eruptions taking place in binary star systems in which a white dwarf accretes material from a non-degenerate stellar companion. After the nova event, a shell of gas is expelled and expands into the surrounding environment at hundreds to thousands of km s^{-1}. This shell, the so-called nova remnant, experiences interactions with the binary system, the accretion disk, the surrounding environment, and very notably with continuous winds from the white dwarf powered by radiation from nuclear burning on its surface. The similarities with the formation of planetary nebulae are obvious, yet the shaping of nova remnants occurs on much shorter time-scales. This results in the prevalent round to mild elliptical 3D shape of nova remnants. Here we describe the morphology, kinematics and dynamics of nova remnants based on our multi-epoch imaging and long-slit and integral field spectroscopic studies and compare them with those of planetary nebulae.

Keywords. Catalogs, Surveys, stars: binaries, planetary nebulae

1. Introduction

The term nova (plural novae) comes from the latin phrase *"stella nova"*†, meaning the presence of a new star in the sky. Novae are actually luminous eruptions taking place in binary systems composed of a white dwarf (WD) and a non-degenerate stellar companion (e.g., Gallagher & Starrfield 1978). The WD accretes material from the companion until its envelope reaches a critical mass and a thermo-nuclear (TNR) event takes place (Starrfield et al. 1972).

There are a great variety of nova types, depending on the nature of the host binary system, the accretion rate, and the accretion history and mode. In a classical nova (CN), the host binary is a cataclysmic variable (CV) with the secondary, typically a main sequence star, in a short-period orbit, P $\approx$ 1.4-10 hours, thus overflowing its Roche lobe (Warner 2003). Meanwhile, in an embedded nova, proposed to be 20-40% of all nova events, most likely including symbiotic novae and luminous red variable, the WD companion is an evolved red giant star in a long-period orbit, P $\gtrsim$ 100 days (Mikolajewska 2010; Tylenda et al. 2011). These two different types of novae differ notably on the accretion modes and circumstellar media (CSM). In classical novae, the accretion onto the WD is channeled through an accretion disk (Bode & Evans 2008) and the CSM has low (or even negligible) density resulting from the high efficiency of the accretion process. On the other hand, in embedded novae, the accretion onto the WD is mainly through

† First time used by the Danish astronomer Tycho Brahe referring (actually) to a supernova, the so-called Tycho's Supernova or Supernova 1572.

direct wind accretion, resulting in a low accretion efficiency that produces a high-density CSM, i.e., the WD (and the nova as well) is embedded within the red giant wind.

1.1. *The Thermo-Nuclear Runaway (TNR) Event*

In pre-outburst, during most of the life-time of the binary system, the WD accretes H-rich material†. Hydrogen burns at the base of the WD envelope stably either through the p-p chain or the ^{3}He-burning reaction at a rate equal to the accretion rate, $\dot{M}_{\rm acc}$. The energy produced at the bottom of the envelope is transported away by radiation and e^- conduction. As time goes by, the envelope mass increases and it also does the density and temperature at its base. This results in a subsequent increase of the energy release rate.

When a critical mass $M_{\rm crit}$ is accreted, the energy release rate becomes too high for radiative and conductive transport of the energy outwards, and the envelope becomes convective. This, in fact, further increases the nuclear burning rate, as fresh, H-rich material is injected into the burning layer. The result is the onset of the so-called Thermo-Nuclear Runaway (TNR).

The TNR is a complex physical process, involving convection, mixing, instabilities, and nuclear processes. It is important to remark that there is no detonation or deflagration, as convection redistributes very efficiently the energy released throughout the envelope. As a result, the thermal energy of the envelope grows until it reaches the gravitational binding energy and expands. This quenches the nuclear burning rate, so that the TNR then enters a prolonged phase of enhanced, steady burning. The energy release and radioactive heating resulting from the release of energy from β-unstable nuclei eject a fraction of the envelope within minutes to hours.

"All novae are recurrent, but some are more recurrent than others." After a classical nova eruption, accretion may undergo a "hibernation period" due to the disruption of the accretion disk, to disk instabilities, to the inhibition of accretion by the WD wind, ... but the system will finally return to the previous accretion conditions (Shara et al. 1986). With time, another TNR will be triggered with a recurrence time

$$\tau_{\rm rec} \approx \frac{M_{\rm crit}}{\dot{M}_{\rm acc}} \quad (1)$$

The critical mass for the TNR trigger $M_{\rm crit}$ ranges from 10^{-7} to $10^{-3} M_\odot$. It is a decreasing function of the WD mass and accretion rate, as higher values of $M_{\rm WD}$ and $\dot{M}$acc imply higher temperatures at the base of the envelope and thus smaller envelope mass for the ignition. There is thus a bias towards the detection of CNe (and recurrent novae) events towards more massive WDs with higher accretion mass rates.

For the particular field of research of planetary nebulae (PNe), it is interesting comparing the case of nova events with born-again PNe. During the post-Asymptotic Giant Branch (post-AGB) phase of their evolution, the central stars of a PN (CSPN) may build a shell of helium with the critical mass to ignite a thermal pulse (Schoenberner 1979; Iben et al. 1983). This so-called very late thermal pulse (VLTP) expands the envelope, which cools dramatically and pushes the CSPN back to the low $T_{\rm eff}$ locus of the Hertzprung-Russell diagram of AGB stars. In a sense, the CSPN is born-again. Meanwhile the incomplete ashes of the He-burning are ejected at high-speeds inside the old PN. This ejecta has high C/O ratio (Miller Bertolami et al. 2006), unlike the products of nova events (Starrfield et al. 1998).

† It is also possible to accrete He-rich material from a degenerate evolved companion, but this seems to have a very low frequency rate, with V445 Pup the most notorious candidate for a helium nova (Ashok & Banerjee 2003).

https://doi.org/10.1017/S1743921324000954 Published online by Cambridge University Press

1.2. *Mass Ejection Modes and Nova Shaping*

The expansion velocity of the ejecta $V_{\rm ej}$ in nova events ranges from 200 to 7000 km s^{-1}. Since the expansion velocity of the ejecta should equal at least the escape velocity from the launching radius, R, this implies

$$V_{\rm ej} \geq V_{\rm esc} = \sqrt{\frac{2GM}{R}}. \quad (2)$$

Assuming the mass of the system is basically that of the WD, which is actually the most massive component, the launching radius has values between the typical WD radii, $R_{\rm WD} \leq 10^9$ cm, and the binary separation

$$a_{\rm bin} = 3.5 \times 10^{10} M^{1/3} P^{2/3} \ ({\rm cm}), \quad (3)$$

where the system mass M is in units of $M_\odot$ and the orbital period P in hours. This suggests that the launching radius is above the surface of the WD, but below the orbital radius of the companion.

Another critical piece of evidence to understand the nova event comes from the early detection of X-rays, which arises from shocks within the ejecta itself. This implies the presence of a slow outflow that is shocked and pushed forward by a fast outflow. Nowadays the most accepted scenario for the nova ejection considers the interaction of a series of stellar winds formed at different times after the TNR.

There is an initial impulsive ejection of mass caused by the TNR. This prompt ejection occurs within a few hours after the TNR is triggered. The mass and velocity of the ejecta depend on the mixing between the envelope and underlying WD core, which can vary largely from case to case, although only a fraction of envelope is expected to be ejected.

This impulsive ejection is followed by a short-lived stellar wind driven by radiation pressure. Its mass-loss rate is known to decline by a factor ≈10 over just a few hours, because otherwise the supersoft X-ray phase of novae would last longer.

Finally this short-lived wind is superseded by a prolonged optically thick wind with terminal velocity $V_{\rm ej} \geq 1000$ km s^{-1}. This speed implies that the launching radius is smaller than the binary separation, close to the WD surface. The wind is indeed driven by radiation pressure, with acceleration taken place deep below the photosphere. The wind driver is actually the Fe opacity bump at $T \approx 1.6 \times 10^5$ K in the nova envelope. As the mass the WD H-rich envelope decreases, owing to nuclear burning and wind loss, the wind mass loss rate $\dot{M}_{\rm w}$ itself decreases. At the same time the photosphere recedes to smaller radii to reach regions of higher temperature, producing the increase of the wind velocity as the wind launching radius moves inward. Once the temperature drops below 1.6×10^5 K, there are no additional sources of opacity and the wind ceases after a time period from a few days to a few months.

The duration of this phase is expected to be longer for WD with lower mass and higher values of critical mass for the TNR ignition. These novae are classified as "slow novae", in opposition to "fast novae", given their slower decay from brightness peak, as measured by t_3, the time it takes to decline 3 mag from the peak brightness. These "slow novae" do not only last longer, but also their ejecta have slower velocity. Nova remnants are thus shped by wind-wind interactions, as much as PNe (Kwok, Purton, & Fitzgerald 1978; Balick 1987).

2. Nova remnants morphology

2.1. *Early Observations*

It is necessary to remark that the early phases of the TNR are very complex. The TNR may not be triggered simultaneously over the full WD envelope layer, resulting in

https://doi.org/10.1017/S1743921324000954 Published online by Cambridge University Press

asymmetric ejecta on small spatial scales. On coherent larger scales, the fast rotation of a WD would produce latitude-dependent variations of the pressure and temperature at the base of the envelope and thus of the TNR. The envelope corotation with the spinning WD surface can be enhanced by magnetic coupling.

At the nova brightness peak, the photosphere of the WD would have expanded largely, up to $10^{12} - 10^{13}$ cm, engulfing the binary system if their orbital period is shorter than 12 hours. This is a scenario similar to a common-envelope phase, well known to occur in PNe (De Marco 2009) and stellar mergers (Ivanova et al. 2013). Therefore processes of frictional drag, binary orbital motion (centrifugal forces), companion's gravity, ... will be active, focusing the mass loss towards the orbital plane, preferentially through the outer L2 Lagrange point, on the far side of the secondary. The binary influence would be greater for slow novae, with $V_{\rm ej} \leq 1000$ km s^{-1} and launching radius of the wind beyond the orbital separation $a_{\rm bin}$.

Early spectral observations of novae in their nebular stage detect double- or triple-peaked line profiles that imply the asphericity in the ejecta. These can be interpreted as a bipolar ejecta and an equatorial torus or disk (Chochol et al. 1997). Early images of nova ejecta are consistent with an elliptical shell whose ellipticity changes with time, becoming either rounder or more prolate. One of the most remarkable cases is that of V959 Mon (a.k.a. nova Mon 2012), whose binary system edge-on inclination favors observing these changes. Indeed, multi-epoch radio images of V959 Mon captured an orthogonal flip in the major axis of the ejecta from a bi-lobed ejecta on day 126 interpreted as a fast bipolar flow to a slower, equatorially concentrated flow on day 615 (Chomiuk et al. 2014). All these are observational evidence of the interaction of two winds or outflows with different symmetry.

Moreover, there are features in spectral lines that persist at a particular velocity. These are believed to originate in discrete clumps, revealing the ejecta clumpy nature. The presence of spectral features around the brightness peak of both low- and high-ionization species also supports a broad range of densities and temperatures within the ejecta, which can result from self-shielding by these clumps.

2.2. *Nova Remnant Morphological Catalog*

Nova ejecta have expansion velocities of a few hundreds up to 1000 km s^{-1}, thus their apparent angular diameter grows so fast

$$\theta = 0.115 \left(\frac{d}{1\ \rm kpc}\right)^{-1} \left(\frac{V_{\rm ej}}{1000\ \rm km\ s^{-1}}\right) \left(\frac{t}{100\ \rm day}\right)\ \rm arcsec \qquad (4)$$

that high-resolution facilities like the *Hubble Space Telescope* (*HST*), near-IR adaptive-optics, and radio/millimeter interferometers can resolve nova ejecta starting a few months to a few years after their eruption. Otherwise ground-based optical imaging would resolve novae from a few years to a few decades after the eruption.

We have undertaken (Santamaría et al. 2024, in prep.) a compilation of archival and proprietary ground-based and *HST* optical narrow-band Hα, Hα+[N II], [N II], and [O III] images of resolved nova remnants. So far this compilation includes images for ≈50 nova remnants with ages from 15 up to 600 years.

Among the nova remnants in this catalog, the most typical morphology is an elliptical shell (see also Slavin, O'Brien, & Dunlop 1995; Gill & O'Brien 1998; Downes & Duerbeck 2000). In a few cases, such RR Pic and HR Del (Figure 1), it is noted an equatorial enhancement (ring), with bipolar over-densities, sometimes observed at different emission lines. Overall the frequency rate of bipolar morphology is very low, with V959 Mon (a NeO

https://doi.org/10.1017/S1743921324000954 Published online by Cambridge University Press

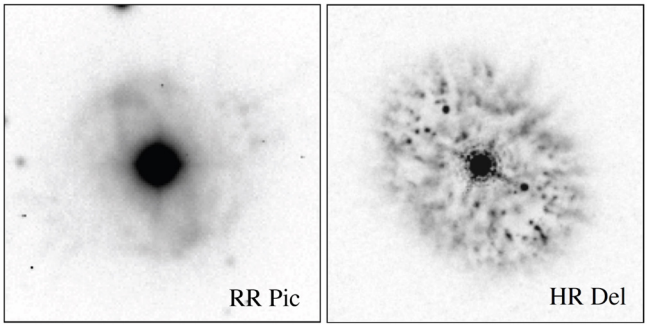

Figure 1. Hα images of the nova remnants RR Pic (left) and HR Del (right). RR Pic shows a clear equatorial enhancement, which is only present in forbidden emission line images of HR Del. Images adopted from the morphological catalog of nova remnants (Santamaría et al. 2024, in preparation).

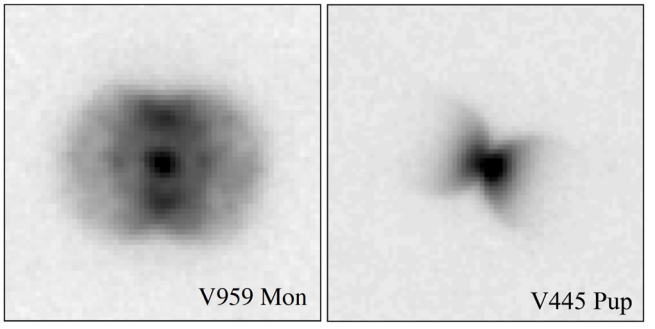

Figure 2. Hα and broad-band images of the bipolar nova remnants V959 Mon (left) and V445 Pup (right), respectively. Images adopted from the morphological catalog of nova remnants (Santamaría et al. 2024, in preparation).

nova detected in GeV γ rays) and V445 Pup (the best candidate for a degenerate, He-donor companion) the only clear cases for this asymmetric morphology (Fig. 2).

In a few other cases the nova remnants exhibit an one-sided clumpy ring, with cometary tail morphology for the individual clumps. The nova remnants IPHASX J210204.7+471015 and AT Cnc (Figure 3) can be thus attributed to an ejection through the L2 point after a common envelope phase (Guerrero et al. 2018; Shara et al. 2012).

There is no clear evidence for fast collimated outflows (jets) in nova remnants, with only a confirmed jet detected in X-rays in DQ Her, probably resulting from the collimation of the current stellar wind (Toalá et al. 2020). Otherwise the jet claimed in GK Per (Shara et al. 2012b) might actually be a section of a larger nebular structure, probably a PN (Harvey et al. 2016).

The detailed morphology of the elliptical shells of nova remnants can be considered smooth, but there is also the presence at different degrees of clumps embedded within those diffuse shells. These clumps shed light into the possible novae yields trapped into clumps, with head and cometary tail morphology that inform on the presence of ablated flows as in GK Per and DQ Her (Liimets et al. 2012; Santamaría et al. 2020; Santamaria et al. 2022a). The comparison of the ALMA interferometric observations of V5668 Sgr ($d = 1450$ pc) with *HST* observations seems actually to imply that novae

https://doi.org/10.1017/S1743921324000954 Published online by Cambridge University Press

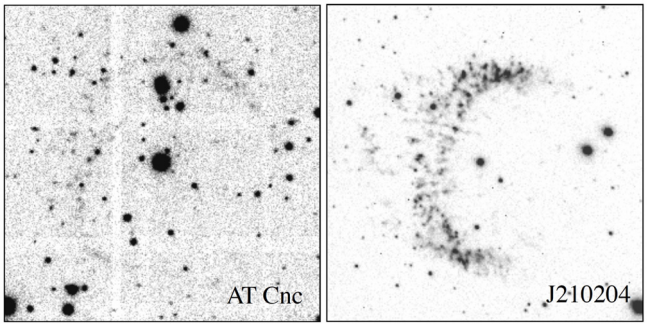

Figure 3. Hα images of the one-sided ring nova remnants AT Cnc (left) and IPHASX J210204.7+471015 (right). Images adopted from the morphological catalog of nova remnants (Santamaría et al. 2024, in preparation).

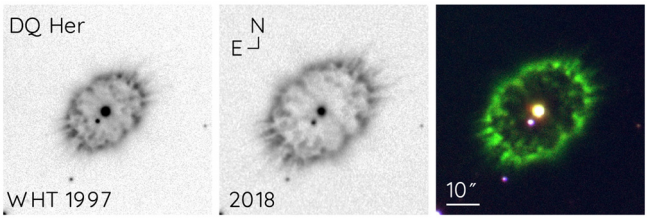

Figure 4. Hα images of DQ Her obtained on 1997 and 2018 at the William Herschel Telescope and Nordic Optical Telescope, respectively. Adopted from Santamaría et al. (2020).

remnants are mostly clumpy, but the limited spatial resolution hinders resolving those clumps, resulting in an apparent smooth morphology (Diaz et al. 2018).

The upcoming morphological catalog of nova remnants will allow us investigating in detail their morphology statistics, and the effects of time-evolution and distance in the observed morphology. There will be soon a dedicated webpage with FITS and JPG files available to the astronomical community. Contributions of images are most welcomed.

3. Angular expansion of nova remnants

The fast angular expansion of nova shells noted in Eq. 4 allows using multi-epoch images of nova remnants to assess their distance, compare the radial and tangential expansion velocity, and their 3D physical structure. It also allows to witness morphological changes.

Notorious examples of multi-epoch imaging of nova remnants that have revealed their expansion are those of DQ Her (a.k.a. Nova Her 1934) based on images from 1977 to 2019, i.e., for a nova age from 43 to 85 years old (see Fig. 4, Santamaría et al. 2020), and GK Per (a.k.a., Nova Per 1901) based on images from 1953 to 2011, i.e., for a nova age from 52 to 110 years old (Liimets et al. 2012). Another well studied cases are those of IPHASX J210204.7+471015 and T Pyx (Santamaría et al. 2019; Schaefer, Pagnotta, & Shara 2010).

We have also undertaken a comprehensive investigation of the expansion of nova shells (Santamaría et al. 2020). A first study has included a sample of five nova remnants with ages in the range from 50 to 130 years. All these have resulted to be in a free expansion phase, with the ejecta mass being 7-45 times larger than the swept-up CSM/ISM medium around the novae (Fig. 5). Combined with the surface brightness decline, it implies that

https://doi.org/10.1017/S1743921324000954 Published online by Cambridge University Press

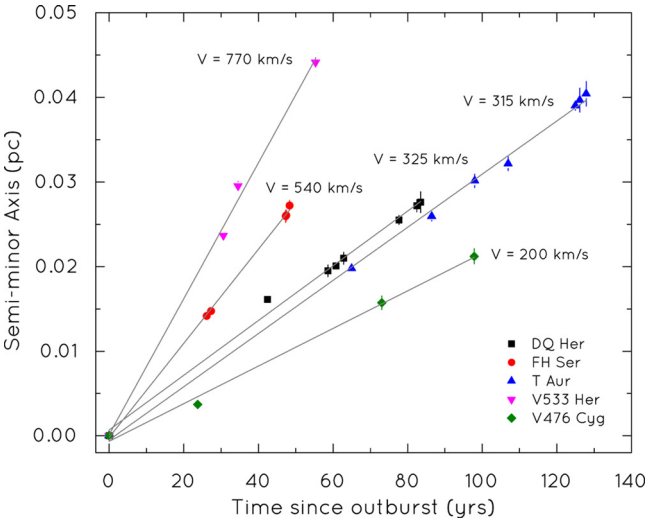

Figure 5. Semi-minor axis expansion of a sample of five nova remnants. The slope determines the tangential velocity on the sky. Adopted from Santamaría et al. (2020).

the life-time of nova remnants is smaller than a few hundred years, with implications for nova remnants dispersal time into ISM and the occurrence of nova events.

It is notorious the case of IPHASX J210204.7+471015 (Santamaría et al. 2019). The [N II]-bright one-sided ring-like feature expands freely, but the [O III] bow-shock-like features seems to have experienced a notable slow down in its interaction with the ISM.

A study based on a larger sample drawn from the morphological catalog of nova remnants is coming soon (Santamaría et al. 2024, in preparation). A preliminary inspection confirms the free expansion of most nova remnants.

4. Physical structure of nova remnants

Angular expansion studies of nova remnants have shown that the radial expansion velocity along the line of sight is not always coincident with the tangential velocity on the plane of the sky (e.g., Slavin, O'Brien, & Dunlop 1995). These differences reveal projection effects, as a shell with elliptical morphology can actually be a tilted oblate or prolate ellipsoid, but also that spectroscopy and multi-epoch imaging probe different structural components, including ring-like structures, outflows, or clumps among others. Otherwise it also unveils errors in distance estimate based on *Gaia* data, as the stellar emission might be contaminated by the "red" nebular emission of the nova remnant, or very notably unreliable radial expansion velocity measurements based in the misleading interpretation of early spectroscopic data.

4.1. *Long-slit Spectroscopic Studies*

Long-slit spectroscopic data along the two main minor and major symmetry axes of nova remnants have proven very efficient to assess their true 3D physical structure (Slavin, O'Brien, & Dunlop 1995). No extreme high-dispersion is required given the fast expansion velocity of nova remnants, with a spectral resolution $R \approx 5000$ being the best trade off between resolution and sensitivity.

A recent long-slit spatio-kinematic investigation of four nova remnants, namely T Aur, DQ Her, QU Vul, and HR Del, and the nova-like source CK Vul (Santamaria et al. 2022a)

https://doi.org/10.1017/S1743921324000954 Published online by Cambridge University Press

has clarified their 3D physical structure. Besides CK Vul, with an hour-glass bipolar morphology, the bona-fide nova remnants in this sample can be described as mild prolate ellipsoidal shells with equatorial density enhancements, that in a few cases (e.g., T Aur) is better described by a peanut-shape with open caps.

The comparison of the unprojected (true) axial ratio of these novae with their expansion velocity and decline time t_3 reveals notorious trends. Slow novae, with longer decline time t_3, have slower expansion velocities and are more aspherical than fast novae. Apparently the slower ejecta of these novae have longer interaction times with the companion star, producing more pronounced effects on their shape (Livio et al. 1990; Lloyd, O'Brien, & Bode 1997) as discussed in Section 1.1.

4.2. *Integral Field Spectroscopic Studies*

Long-slit spectroscopic studies of nova remnants are largely superseded by integral field spectroscopic (IFS) observations. These provide a complete spatial coverage, which is essential to identify the symmetry axes and to resolve small-scale (filaments, clumps) structures embedded in the nebular shell (or may be even being its main structural component).

The IFS instrument MEGARA (Gil de Paz et al. 2016) at the GTC 10.4m telescope is well suited for this task. With a spectral resolution up to 18700 in the Hα line, for a velocity resolution $\approx$16 km s^{-1}, it can provide a truly tomographic view of nova remnants. This has been tested with QU Vul, which shows nebular Hα emission in the range from -616 to $+664$ km s^{-1}. Its 3D physical structure is shown to consists of a prolate ellipsoid with axial ratio 1.4$\pm$0.2, inclination with the line of sight $12^\circ \pm 6^\circ$, and polar and equatorial velocities of 560 km s^{-1} and 400$\pm$60 km s^{-1}, respectively (Santamaría et al. 2022b). This greatly improves the morpho-kinematic model obtained by Santamaria et al. (2022a) using a long-slit spectrum.

The tomographic view of QU Vul helps greatly to interpret many different aspects (Fig. 6). For instance, the ionized mass can be derived from the Hα flux at each spatio-kinematic element of the IFS data cube, thus reducing the uncertainty associated to the macroscopic filling factor. The determination of the kinetic energy benefits both from the more accurate value of the ionized mass and from the assessment of the space velocity on each data cube element as well.

Moreover the integrated nebular Hα line profile shows a "castellated" shape (Fig. 7), which is typically seen in early spectroscopic observations of novae. The peaks in the profiles, i.e., the "battlements in the wall of the castle" of this profile, can be unambiguously associated with individual knots moving along radial directions with different inclinations with the line of sight. The association of profile peaks with clumps allows an accurate determination of the expansion velocity, which is typically overestimated on early spectroscopic observations of nova ejecta that assumes either

$$V_{\rm exp} \;=\; FWHM \tag{5}$$

or more geometrically exact

$$V_{\rm exp} \;=\; \frac{FWHM}{2\sqrt{\ln 2}} \;=\; 0.72 \times FWHM \tag{6}$$

but can be defined more precisely by the semi-difference between the velocities of the bluest and reddest profile peaks

$$V_{\rm exp} \;=\; \frac{V_{\rm red} - V_{\rm blue}}{2}. \tag{7}$$

https://doi.org/10.1017/S1743921324000954 Published online by Cambridge University Press

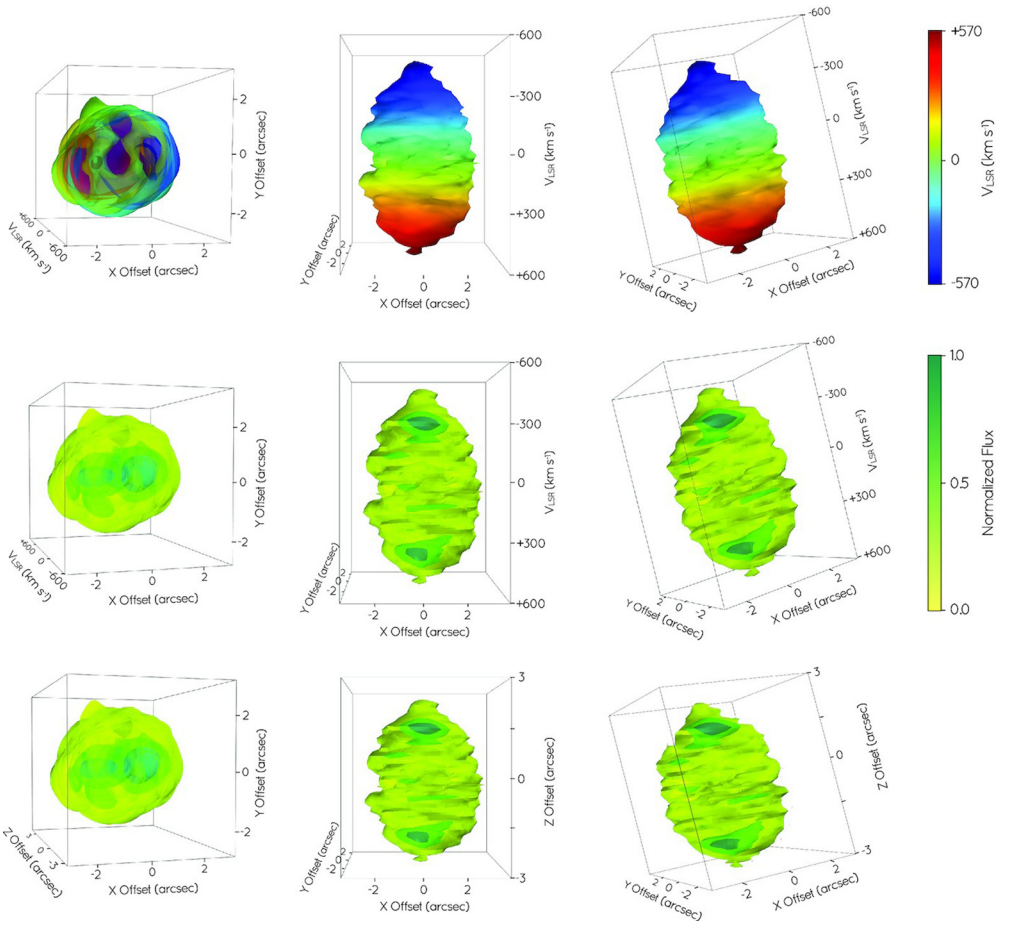

Figure 6. Hα emission velocity-coloured (top) and intensity (middle) position-position-velocity (PPV) diagrams of QU Vul, and true 3D intensity distribution (bottom) along the observer's point of view (i.e. the direct image, left), and the projection from the plane of the sky along directions orthogonal (middle) and parallel (right) to the main axis. Adopted from Santamaría et al. (2022b).

Finally note that the Hα decline of QU Vul implies that the nova remnant will be not detectable in a short time period of 40-60 years from now.

5. Concluding Remarks

The expansion and morphological evolution of nova remnants can be followed from a few years up to a few hundred years after the nova eruption. The expansion of nova remnants is not slowed down by their interaction with the tenuous CSM around them or the surrounding ISM. The importance of binary shaping effects in the nova remnants differs among nova types, being larger in those with slow expansion velocities. On the other hand it is noted that clumping may dominate nova remnants, with nova yields trapped into clumps.

Nova remnants and PNe are both shaped by wind-wind interactions, but it takes much shorter time-scales, from hours to months, in the former. As many PNe, nova remnants are shaped by binary interactions, but most nova remnants have mild ellipsoidal 3D

https://doi.org/10.1017/S1743921324000954 Published online by Cambridge University Press

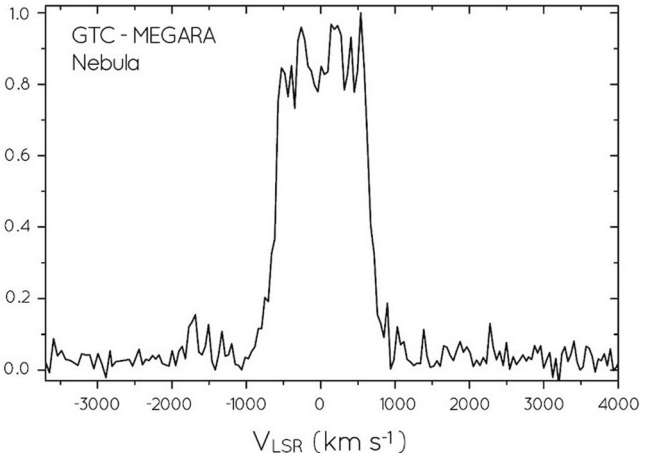

Figure 7. Hα emission line profile of the nebular emission of QU Vul detected by GTC MEGARA. The spectral line profile has a flat, 'castellated' top. Adopted from Santamaría et al. (2022b).

shapes with very few bipolar and even less show jets. This results from the binary shaping effects diluting in short time-scales in nova remnants. The time dilution of nova remnants, $\approx$200 years, is much shorter than in PNe. In a sense, nova remnants are fast-forward PNe, but the longer different time-scale of the wind-wind interactions in PNe makes their morphology more inclined to depart from spherical symmetry.

We deeply appreciate the collaboration of Drs. Sara Cazzoli, Gerardo Ramos-Larios, Laurence Sabin and Jesús A. Toalá to the results based on multi-epoch imaging and spectroscopic observations of nova remnants described here. MAG acknowledges financial support from grants CEX2021-001131-S funded by MCIN/AEI/10.13039/501100011033 and PGC 2018-102184-B-100 and PID 2022-142925NB-I00 from the Spanish Ministerio de Ciencia, Innovación y Universidades (MCIU) cofunded with FEDER funds. MAG also warmly acknowledges funding support provided by the Local Organizing Committee of the International Astronomical Union Symposium 384.

References

Ashok N. M., Banerjee D. P. K., 2003, A&A, 409, 1007. doi:10.1051/0004-6361:20031160
Balick B., 1987, AJ, 94, 671. doi:10.1086/114504
Bode M. F., Evans A., 2008, clno.book
Chochol D., Grygar J., Pribulla T., Komzik R., Hric L., Elkin V., 1997, A&A, 318, 908
Chomiuk L., Linford J. D., Yang J., O'Brien T. J., Paragi Z., Mioduszewski A. J., Beswick R. J., et al., 2014, Natur, 514, 339. doi:10.1038/nature13773
De Marco O., 2009, PASP, 121, 316. doi:10.1086/597765
Diaz M. P., Abraham Z., Ribeiro V. A. R. M., Beaklini P. P. B., Takeda L., 2018, MNRAS, 480, L54. doi:10.1093/mnrasl/sly121
Downes R. A., Duerbeck H. W., 2000, AJ, 120, 2007. doi:10.1086/301551
Gallagher J. S., Starrfield S., 1978, ARA&A, 16, 171. doi:10.1146/annurev.aa.16.090178.001131
Gil de Paz A., Carrasco E., Gallego J., Iglesias-Páramo J., Cedazo R., García Vargas M. L., Arrillaga X., et al., 2016, SPIE, 9908, 99081K. doi:10.1117/12.2231988
Gill C. D., O'Brien T. J., 1998, MNRAS, 300, 221. doi:10.1046/j.1365-8711.1998.01899.x
Guerrero M. A., Sabin L., Tovmassian G., Santamaría E., Michel R., Ramos-Larios G., Alarie A., et al., 2018, ApJ, 857, 80. doi:10.3847/1538-4357/aab669

Harvey E., Redman M. P., Boumis P., Akras S., 2016, A&A, 595, A64. doi:10.1051/0004-6361/201628132
Iben I., Kaler J. B., Truran J. W., Renzini A., 1983, ApJ, 264, 605. doi:10.1086/160631
Ivanova N., Justham S., Chen X., De Marco O., Fryer C. L., Gaburov E., Ge H., et al., 2013, A&ARv, 21, 59. doi:10.1007/s00159-013-0059-2
Kwok S., Purton C. R., Fitzgerald P. M., 1978, ApJL, 219, L125. doi:10.1086/182621
Liimets T., Corradi R. L. M., Santander-García M., Villaver E., Rodríguez-Gil P., Verro K., Kolka I., 2012, ApJ, 761, 34. doi:10.1088/0004-637X/761/1/34
Livio M., Shankar A., Burkert A., Truran J. W., 1990, ApJ, 356, 250. doi:10.1086/168836
Lloyd H. M., O'Brien T. J., Bode M. F., 1997, MNRAS, 284, 137. doi:10.1093/mnras/284.1.137
Mikolajewska J., 2010, arXiv, arXiv:1011.5657. doi:10.48550/arXiv.1011.5657
Miller Bertolami M. M., Althaus L. G., Serenelli A. M., Panei J. A., 2006, A&A, 449, 313. doi:10.1051/0004-6361:20053804
Santamaría E., Guerrero M. A., Ramos-Larios G., Sabin L., Vázquez R., Gómez-Muñoz M. A., Toalá J. A., 2019, MNRAS, 483, 3773. doi:10.1093/mnras/sty3364
Santamaría E., Guerrero M. A., Ramos-Larios G., Toalá J. A., Sabin L., Rubio G., Quino-Mendoza J. A., 2020, ApJ, 892, 60. doi:10.3847/1538-4357/ab76c5
Santamaría E., Guerrero M. A., Zavala S., Ramos-Larios G., Toalá J. A., Sabin L., 2022a, MNRAS, 512, 2003. doi:10.1093/mnras/stac563
Santamaría E., Guerrero M. A., Toalá J. A., Ramos-Larios G., Sabin L., 2022b, MNRAS, 517, 2567. doi:10.1093/mnras/stac2789
Schaefer B. E., Pagnotta A., Shara M. M., 2010, ApJ, 708, 381. doi:10.1088/0004-637X/708/1/381
Schoenberner D., 1979, A&A, 79, 108
Shara M. M., Livio M., Moffat A. F. J., Orio M., 1986, ApJ, 311, 163. doi:10.1086/164762
Shara M. M., Mizusawa T., Wehinger P., Zurek D., Martin C. D., Neill J. D., Forster K., et al., 2012, ApJ, 758, 121. doi:10.1088/0004-637X/758/2/121
Shara M. M., Zurek D., De Marco O., Mizusawa T., Williams R., Livio M., 2012, AJ, 143, 143. doi:10.1088/0004-6256/143/6/143
Slavin A. J., O'Brien T. J., Dunlop J. S., 1995, MNRAS, 276, 353. doi:10.1093/mnras/276.2.353
Starrfield S., Truran J. W., Sparks W. M., Kutter G. S., 1972, ApJ, 176, 169. doi:10.1086/151619
Starrfield S., Truran J. W., Wiescher M. C., Sparks W. M., 1998, MNRAS, 296, 502. doi:10.1046/j.1365-8711.1998.01312.x
Toalá J. A., Guerrero M. A., Santamaría E., Ramos-Larios G., Sabin L., 2020, MNRAS, 495, 4372. doi:10.1093/mnras/staa1502
Tylenda R., Kamiński T., Schmidt M., Kurtev R., Tomov T., 2011, A&A, 532, A138. doi:10.1051/0004-6361/201116858
Warner B., 2003, cvs..book, 592. doi:10.1017/CBO9780511586491